

# **La<sup>3+</sup>-induced (micro)structural changes and origin of the relaxor-like phase transition in ferroelectric lead barium niobate electroceramics**

Michel Venet<sup>a\*</sup>, Fabio L. Zabotto<sup>a</sup>, Jose E. Garcia<sup>b</sup>, Diego A. Ochoa<sup>b</sup>,  
Ducinei Garcia<sup>a</sup>, José A. Eiras<sup>a</sup>, Jean-Claude M'Peko<sup>c</sup>

<sup>a</sup> *Departamento de Física, Universidade Federal de São Carlos (UFSCar), CEP: 13565-670 São Carlos - SP, Brazil. Email: [venet74@df.ufscar.br](mailto:venet74@df.ufscar.br). Phone: +55 16 33519731*

<sup>b</sup> *Departament de Física Aplicada, Universitat Politècnica de Catalunya, Barcelona, Spain.*

<sup>c</sup> *Instituto de Física de São Carlos (IFSC), Universidade de São Paulo (USP), C. Postal: 369, CEP: 13560-970 São Carlos - SP, Brazil.*

## **Abstract**

Lead barium niobate ( $\text{Pb}_{1-x}\text{Ba}_x\text{Nb}_2\text{O}_6$ , PBN) ferroelectric materials have been and are the subject of numerous studies in literature due to their potential for wide-ranging applications in the electronic industry. In this work, La<sup>3+</sup>-doped  $\text{Pb}_{0.56}\text{Ba}_{0.44}\text{Nb}_2\text{O}_6$  (PBN44) electroceramics were prepared and investigated in terms of X-ray diffraction, scanning electron microscopy, thermal spectra of dielectric permittivity, Curie-Weiss law and hysteresis loop characteristics. It was noted that La<sup>3+</sup> doping favors the formation of orthorhombic *mm2* phase in PBN44, which originally shows only the tetragonal *4mm* symmetry-related phase. In particular, the PBN44 material with 1 wt.%  $\text{La}_2\text{O}_3$  displays (micro)structural characteristics and dielectric properties similar to those from PBN compositions lying within their morphotropic phase boundary region. Our results also show that La<sup>3+</sup> is able to promote a change of the ferroelectric to paraelectric phase transition appearance of PBN44 from pseudo-normal to really diffuse. However,

conversion to a diffuse plus relaxor transition behavior reveals directly linked to incommensurate superstructures present and dielectrically-active in PBN materials toward low temperatures, with an intrinsically frequency-dispersive dielectric response. This statement is also supported by observation of hysteresis loops showing a transformation trend to pseudo-slim-like, even in the normal-like ferroelectrics, when moving into the temperature region of incommensuration manifestation.

Keywords: PBN, diffuse phase transition, tungsten bronze, hysteresis, Curie Weiss, permittivity.

## 1. Introduction

Lead barium niobate,  $\text{Pb}_{1-x}\text{Ba}_x\text{Nb}_2\text{O}_6$  (PBN), solid solutions belong to the group of ferroelectric niobates with tetragonal tungsten bronze (TTB)-type structure and recognized potential for a wide range of applications in the electronic industry, including the manufacture of electro-optic, nonlinear optic, piezoelectric and pyroelectric devices [1-2]. Originally,  $\text{PbNb}_2\text{O}_6$  (PN) transforms from paraelectric tetragonal  $4/mmm$  to ferroelectric orthorhombic  $mm2$  point group at around 823 K [3-5]. When doped with  $\text{Ba}^{2+}$  cations, the ferroelectric phase of the PBN solutions changes from the above orthorhombic  $mm2$  to tetragonal  $4mm$  symmetry while increasing  $\text{Ba}^{2+}$  content [4,5]. In terms of dielectric response, on the other hand, while undoped PN presents a normal-like, sharp ferroelectric to paraelectric phase transition at a discrete and frequency-independent temperature, known as Curie temperature ( $T_C$ ), a diffuse plus relaxor phase transition (DRPT), typified by a broadening of the transition together with observation of a frequency-dependent  $T_C$  behavior, can be induced through doping.

In literature, the issue of DRPT origin in ferroelectrics has so far attracted the attention of scientists from both the fundamental science and materials research viewpoints [6-9]. In particular, some works have been aimed at finding and trying to

account for the composition-related crossover from diffuse and/or relaxor to normal behaviors in different ferroelectric systems [7-9]. In any case, as a matter of fact, dopant-induced structural disorder, supposedly leading to compositional fluctuations and formation of polar nano-regions (PNRs) with locally different  $T_C$ , is considered to be the very common feature of ferroelectrics with DRPT [6-9]. Nevertheless, despite the remarkable progress achieved in the recent years, the several models to date proposed to account for the cause and mechanisms of PNRs formation [8] are promising but have provided as yet only a partial understanding of this issue. In consequence, some key questions, including the possible prediction of the critical value of dopant content that would be expected for the strength of disorder to induce DRPT, are currently still open to debate. In the present work, a systematic study on the evolution of  $\text{La}^{3+}$ -doped  $\text{Pb}_{0.56}\text{Ba}_{0.44}\text{Nb}_2\text{O}_6$  ferroelectrics from normal to diffuse/relaxor behavior was conducted through considering dielectric and hysteresis loop measurements, with the purpose of trying to closely delineate origin of such transformation events in these materials. For this, we considered beginning our study by performing an analysis of the structural and microstructural characteristics of these materials after sintering, in order to examine possible direct correlations, if any, with their dielectric responses.

## 2. Experimental

$\text{Pb}_{1-x}\text{Ba}_x\text{Nb}_2\text{O}_6$  (with  $x=0.44$ , denoted as PBN44) and  $\text{La}^{3+}$ -doped PBN44 (PBN44 +  $x$  wt.%  $\text{La}_2\text{O}_3$  with  $x = 0.5, 1.0, 1.5, 2.0$  and  $4.0$ , denoted as PBLN44/ $x$ ) ceramic samples were prepared by the conventional method, and sintered at 1270–1290 °C for 2h, as previously reported [10], resulting in bodies with densities above 95% of theoretical density. These specimens were structurally and microstructurally characterized at room temperature through X-ray diffraction (XRD), the measurements of which were performed

using a Rigaku Rotaflex RU200B diffractometer, with  $\text{CuK}\alpha$  radiation, and scanning electron microscopy (SEM) by using a Jeol 5400 LV microscope, the images being obtained on as-sintered samples, without the need of polishing. In addition, for dielectric characterization, platinum electrodes were sputtered on the major surfaces of the ceramic materials. The real and imaginary parts of dielectric permittivity ( $\epsilon'$  and  $\epsilon''$ , respectively) were recorded over wide frequency (20 Hz to 1 MHz) and temperature (15 to 900 K) ranges by using an Agilent 4284A precision LCR meter and an ARS (DE-202SI) cryogenic system. Finally, hysteresis loops from these ceramic samples were measured at a frequency of 60 Hz and electric fields up to  $\sim 3$  kV/mm (found to be enough to reach saturation), using a standard Sawyer-Tower circuit, from high to  $\sim 125$  K. Samples were placed in a nitrogen bath cryostat for low temperature hysteresis loop measurements.

### 3. Results and discussion

Fig. 1 depicts the room-temperature XRD patterns of all the sintered PBLN44/ $x$  specimens, including a magnification of the data around two specific reflection angles of interest for comparison and discussion (right-side graphs). In general, all the patterns showed reflection peaks characteristic of the tetragonal  $4mm$  phase of the PBN system (JCPDS 34-0375), examples of which are the (002) and (551) reflections identified in these magnified graphs at  $2\theta=45.49$  and  $56.85^\circ$ , respectively. In addition, for the compositions with  $x \geq 0.5$ , appearance of two additional peaks, overlapped with those mentioned just above, are noticed in these graphs. These new peaks are better resolved with increasing  $\text{La}_2\text{O}_3$ , because of better peaks splitting, and become finally well-defined at  $2\theta=46.50$  and  $57.30^\circ$  for the spectrum corresponding to the sample with  $x=4.0$ . These peaks were identified as being, respectively, the (004) and (11 1 0) reflections from the orthorhombic  $mm2$  phase of the PBN system. A comparison of the relative intensity of

these additional peaks suggests that the phase fraction with orthorhombic  $mm2$  symmetry increases in these ceramic materials with raising the  $\text{La}_2\text{O}_3$  content, especially for  $x \geq 1.0$ . Both formation and increase of this phase are indicative of an effective incorporation process of  $\text{La}^{3+}$  substituting for  $\text{Pb}^{2+}$  and/or  $\text{Ba}^{2+}$  in the tungsten bronze structure, a process of which is expected to cause distortions of the original PBN crystalline lattice, and may probably also have an important impact on the dielectric properties of these materials, as will be discussed in detail later.

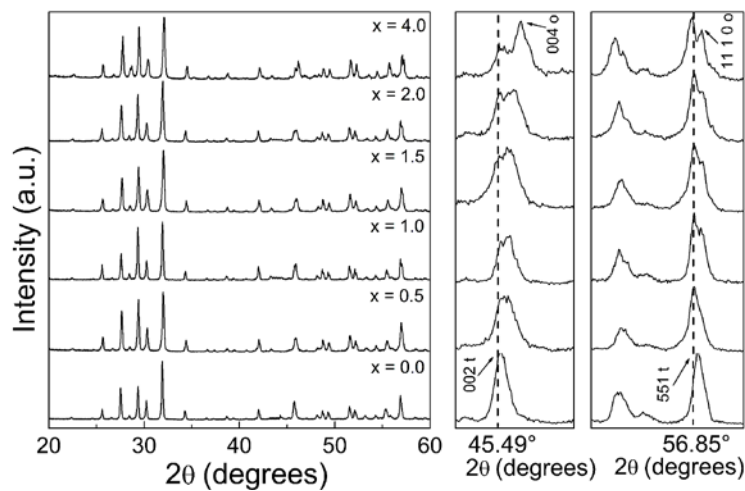


**Figure 1.** Room-temperature XRD patterns of the PBLN44/ $x$  ceramic samples. The symbols “t” and “o” stand for the tungsten bronze phase with tetragonal  $4mm$  and orthorhombic  $mm2$  symmetries, respectively. JCPDS cards 34-0375 and 25-0069 were used to identify the peaks of  $4mm$  and  $mm2$  symmetries, respectively.

The micrographs of the PBLN44/ $x$  ceramics are illustrated in Fig. 2, showing microstructures that consist of grains with a columnar-like morphology. For reference, all the images in this figure involve an identical bar of  $5 \mu\text{m}$ . A somewhat complex behavior of grain size upon variation of  $\text{La}_2\text{O}_3$  content is there noted. That is, the grain size decreases from  $x=0.0$  (Fig. 2(a)) to  $x=0.5$  (Fig. 2(b)). In the following, nevertheless, the ceramic material with the composition  $x=1.0$  (Fig. 2(c)) shows a remarkable increase of the average grain size, together with an increase in the aspect ratio of the grains, which is defined as the length/width ratio. In passing, the microstructures from these samples

( $0.0 \leq x \leq 1.0$ ) were characterized by a trend of showing grains with rounded transversal surfaces, a few examples of which are indicated with the number 1 in Fig. 2(a)-(c)). For the samples with  $x > 1.0$  (Fig. 2(d)-(f)), the grain size undergoes a noticeable decrease again, while the microstructures show to be now composed of grains with rectangular (to hexagonal-like) transversal surfaces, a few examples of which are indicated with the number 2 in this Fig. 2(d)-(f)). This result, i.e., the change in average grain size and transversal surface shape, is to be associated with the increase of the phase fraction with orthorhombic  $mm2$  symmetry, as commented above from the XRD results (Fig. 1), reaching a sufficient proportion as to modify the microstructural characteristics of the prepared ceramics.

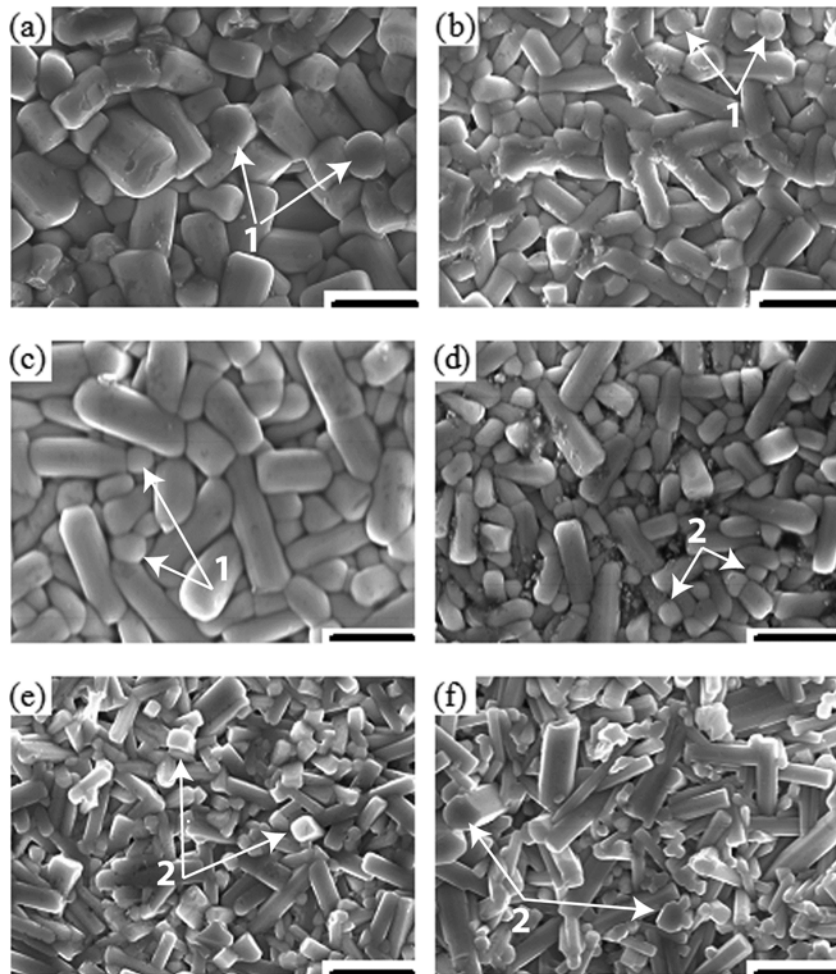


**Figure 2.** Micrographs of the PBLN44/ $x$  ceramic samples: (a)  $x=0.0$ , (b)  $x=0.5$ , (c)  $x=1.0$ , (d)  $x=1.5$ , (e)  $x=2.0$ , and (f)  $x=4.0$ . The bar in all these images represents 5  $\mu\text{m}$ .

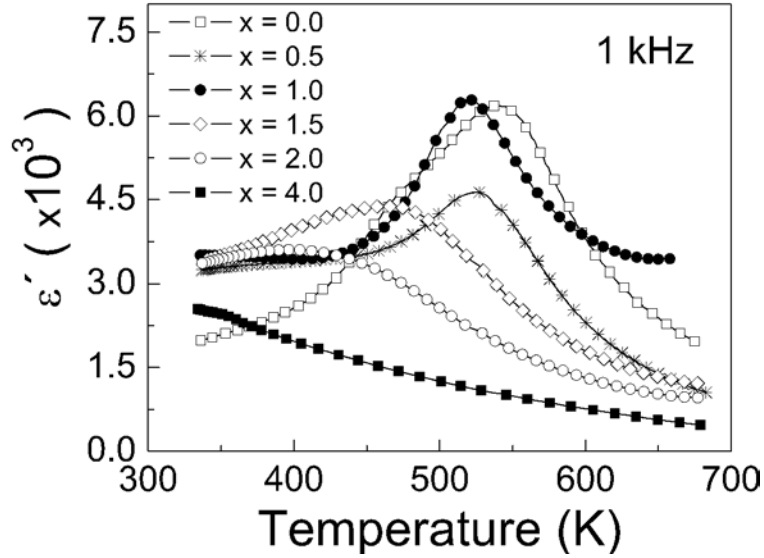


**Figure 3.** Temperature dependence of the real part of dielectric permittivity for the PBLN44/ $x$  ceramic samples, at 1 kHz.

Fig. 3 illustrates the temperature dependence of the real part of dielectric permittivity ( $\epsilon'$ ) for all the PBLN44/ $x$  ceramic samples, as measured at 1 kHz. A quick look at this figure allows concluding, as was expected from literature [11], that the temperature of maximum permittivity ( $T_m \equiv T_C$ ) decreases with increasing the  $\text{La}_2\text{O}_3$  content. For a close analysis, nevertheless, we choose in Fig. 4 to show in detail the behavior of not only  $T_C$  but also maximum permittivity ( $\epsilon'_m$ ) upon variation of the  $\text{La}_2\text{O}_3$  content. (The data for the specimen with the composition  $x=4.0$  do not appear in this figure as its dielectric peak lies below the temperature region covered in Fig. 3, but will be analyzed later in this report.) A clear change in the rate of  $\text{La}^{3+}$ -induced variation of  $T_C$  is noticed in Fig. 4 at  $x=1.0$ , while  $\epsilon'_m$  shows a complex behavior involving a decrease from  $x=0.0$  to  $x=0.5$ , followed by an increase for  $x=1.0$  and, again, a decrease for  $x>1.0$ . While the changes in  $T_C$  should most likely be related to the increasing amount of the orthorhombic phase in the system (as commented above with respect to Fig. 1), so as causing a drop of this property especially for  $x \geq 1.0$ , we note that the changes in  $\epsilon'_m$  reproduce well the behavior observed for the average grain size (refer also to the

microstructure analysis above with respect to Fig. 2). These facts are indicative of the existence of some correlation between dielectric properties and (micro)structural characteristics, as further analyzed just below in light of available literature.

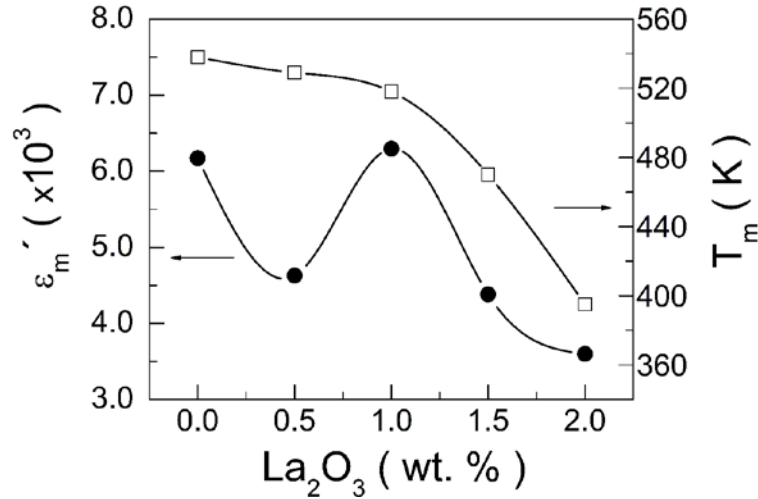


**Figure 4.** Dependence of maximum permittivity ( $\epsilon'_m$ ) and Curie temperature ( $T_m \equiv T_C$ ) on  $\text{La}_2\text{O}_3$  dopant content in the PBLN44/ $x$  samples.

It is well-known that the PBN ferroelectric system presents, in its phase diagram, a morphotropic phase boundary (MPB) region around the PBN37 composition [12], and that ferroelectric materials with MPB have their dielectric and piezoelectric properties enhanced toward this region, where the coexistence of two (or more) ferroelectric phases is characteristically verified. In PBN, particularly, the maximum values of  $\epsilon'_m$  are found in the  $\text{PBN}37 \leq \text{PBN} \leq \text{PBN}40$  composition range [12], toward which, interesting, the maximum values of average grain size are also detected [13], as equally found in this work for PBLN44/1.0. In other words, although the PBN44 lies within the tetragonal region of the phase diagram,  $x=1.0$  seemingly results in an appropriate amount of  $\text{La}_2\text{O}_3$  that makes this material having the (micro)structural characteristics (coexistence and, especially, relative fractions of the tetragonal  $4mm$  and orthorhombic  $mm2$  phases,



included) and dielectric properties similar to those found in the MPB-related  $\text{PBN}_{37} \leq \text{PBN} \leq \text{PBN}_{40}$  composition region.

On the other hand, a quick look at Fig. 3 also allows realizing that, although the ferroelectric to paraelectric phase transition in  $\text{PBN}_{44}$  looks like somewhat diffuse (broadened), increasing the  $\text{La}_2\text{O}_3$  content favors further this behavior (for more precision, results from Curie-Weiss law analysis are given later). This fact is supposed to arise, according to literature on origin of phase transition diffusivity in ferroelectrics [6-9], from dopant-induced structural disorder (which should here, perhaps mainly, involve the structure distortions caused by  $\text{La}^{3+}$ , as we commented above with respect to the XRD results) and development of compositional fluctuations in the PBN system, so as giving rise to (increased) minute regions with locally different  $T_C$ . In fact, the influence of  $\text{La}^{3+}$  on the structure, microstructure and crossover from normal to diffuse phase transition in perovskite structured ferroelectrics has been widely studied [14-16]. In  $\text{La}^{3+}$  doped lead titanate (PLZT), for instance, with the increment of La content, the crystalline structure changes from the ferroelectric rhombohedra phase to the MPB phase, then to the ferroelectric tetragonal phase, finally to the pseudo-cubic phase. La doping in ferroelectric perovskite is believed to disturb the long-rang coulomb interaction and decrease the tetragonal degree, which drives the phase transition and the formation of spontaneous polarization. [17]. Therefore, Lanthanum modified lead zirconate titanate exhibits a diffuse phase transition (DPT) in the dielectric properties for compositions in both the rhombohedral and tetragonal phases. Above a critical lanthanum content (4 at.% for rhombohedral PZT (65/35) and 12 at.% for tetragonal PZT (40/60)), normal micrometer-sized ferroelectric domains cannot be sustained. For high lanthanum- content compositions, sufficiently strong decoupling results in the stabilization of nanometer-sized local polar regions (polar nanodomains). Correspondingly, the macroscopic properties

change from normal ferroelectric to relaxor ferroelectric types with increasing lanthanum content [18-20].

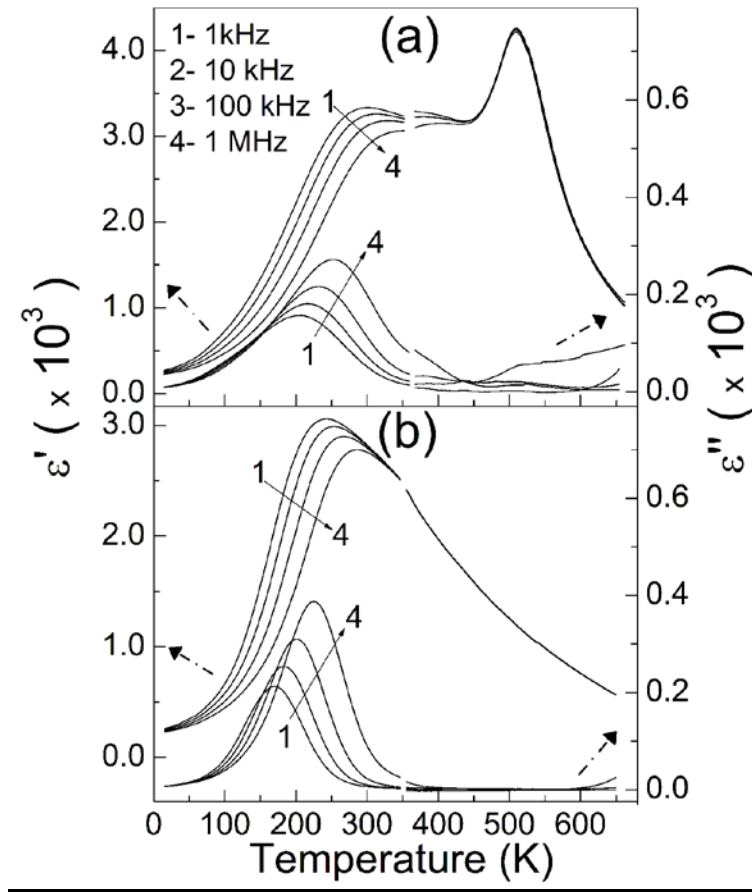


**Figure 5.** Temperature dependences of permittivity ( $\epsilon'$  and  $\epsilon''$ ) for  $\text{La}^{3+}$ -doped PBN44: (a) PBLN44/0.5 and (b) PBLN44/4.0, at various measuring frequencies.

The next point of interest in this work was to closely analyze whether this  $\text{La}^{3+}$  influence can also promote or not relaxor phase transition appearance in PBLN. According to a recent report by the present authors [21], this seemed not to be the case, at least, not in terms of direct link. For that reason, i.e., as a reference that will certainly help introducing and advancing the discussion on origin of diffuse plus relaxor phase transition (DRPT) in such PBN-based materials, we choose to begin summarizing in Fig. 5 the thermal spectra of real ( $\epsilon'$ ) and imaginary ( $\epsilon''$ ) parts of dielectric permittivity found, for instance, for PBLN44/0.5, Fig. 5(a), and PBLN44/4.0, Fig. 5(b). The figure deals with measurements performed at different frequencies and over a larger temperature range. In Fig. 5(a), a

basically frequency-independent dielectric peak is observed around  $T_C=500$  K, a result which is in line with the fact that PBN materials are well known to be normal-like ferroelectrics [22]. The second anomaly appearing in this Fig. 5(a) over a temperature range around 225 K is also observed in PBN materials [21,23], being ascribed to incommensurate superstructures (ICS) that develop in these TTB-structured compounds [5,22]. This anomaly should not be confused with a dielectrically less intense one, not appreciable in this figure, that appears toward lower temperatures (in the 100 to 150 K range [21,23]), and attributed to a phase transition from tetragonal  $4mm$  or orthorhombic  $mm2$  (depending on  $Ba^{2+}$  versus  $Pb^{2+}$  content) to monoclinic  $m$  symmetry [24].

Development of ICS in TTB-structured ferroelectrics has been postulated to arise from displacive structural changes involving defects-associated ferroelastic oxygen octahedral tilting [22,25-26]. Doping PN with  $Ba^{2+}$  and  $La^{3+}$  has the effect of promoting an increase of the ICS magnitude and temperature region of dielectric expression [21], probably owing to dopant versus foreign cations size mismatch, a fact which should modify the above-mentioned ferroelastic tilting and, thus, ICS structural and dipolar dynamics. It can be noted in Fig. 4(a) that the ICS-related dielectric dispersion reveals to be originally of diffuse plus relaxor nature, as reported elsewhere [23-24]. In PBLN44/4.0 (Fig. 5(b)) the decrease of  $T_C$  with  $La^{3+}$  content occurs as noticeable as to the point of dislocating into the temperature region of ICS dielectric expression. In consequence, the PBLN44/4.0 compound develops into a ferroelectric material with a really strong DRPT character. These and other results from our work on doped PN materials allowed us to postulate that the DRPT features observed in PBLN44/4.0 appears to really be a direct consequence of ICS expression [21]. Coincidentally, there exist in the literature some works suggesting, in fact, an apparent connection between DRPT incidence with ICS in other TTB-structured ferroelectrics [27,28].

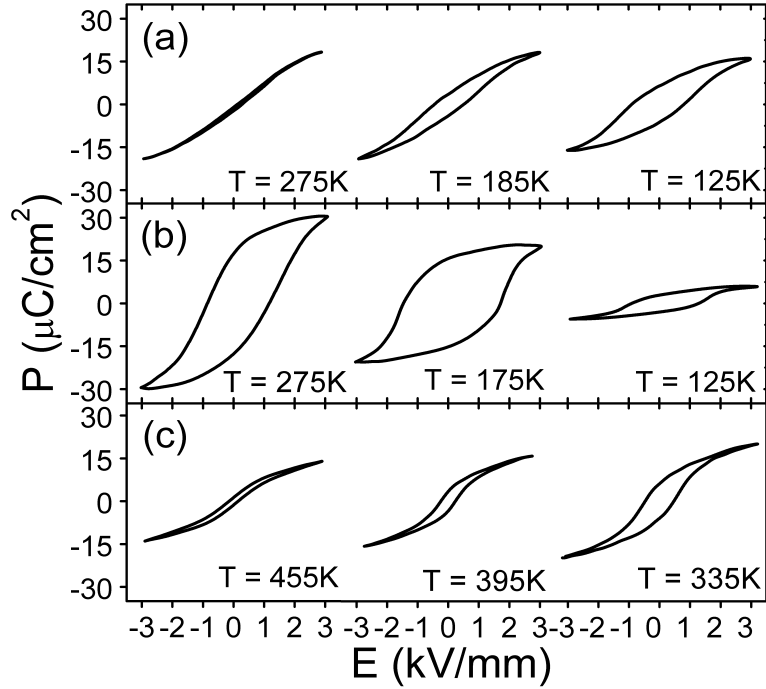


**Figure 6.** Temperature-dependent hysteresis loops for (a) PBLN44/4.0, (b) PBN44 and (c) PBLN44/0.5.

To get further insights into this issue, we chose to proceed with characterization of the materials in terms of ferroelectric hysteresis loops, which are known to be the determinative feature of ferroelectric phases. Fig. 6(a)-(b) depicts the polarization-electric field (P-E) curves measured for PBLN44/4.0 and original PBN44 (PBLN44/0.0) at some representative temperatures. Between 275 and 125 K, the coercive field  $E_c$ , obeying  $P(E_c) \equiv 0$ , showed in both cases the expected trend to increase on cooling, indicating some difficulty of ferroelectric domains reversal when moving toward a frozen-like ferroelectric state. Concretely, nevertheless, while for PBLN44/4.0  $E_c$  continuously increased from 0.01 kV/mm at 275 K to 0.91 kV/mm at 125 K, for PBN44  $E_c$  increased from 1.15 kV/mm at 275 K to 1.95 kV/mm at 175 K, but suffered a sudden and significant decrease to 1.40 kV/mm at 125 K. Of great significance are also the temperature variations of remnant polarization  $P_r$ , where  $P_r \equiv P(E=0)$ , of these PN-based materials, as illustrated in Fig. 7. As predictable for relaxor ferroelectrics [29-30], slim-like hysteresis loops are observed for

PBLN44/4.0 close to the ferroelectric to paraelectric DRPT temperature region (Fig. 6(a)) indicating an inability of the material to sustain macroscopic ferroelectric polarization. On cooling,  $P_r$  naturally shows a trend to moderately increase (Fig. 7). For PBN44, on the other hand, square-like hysteresis loops are observed toward high temperatures (Fig. 6(b)) as also typical of ordinary ferroelectrics [29,30]. For this material, nevertheless,  $P_r$  in Fig. 7 shows a gradual decrease followed by some collapse and, thereby, observation in Fig. 6(b) of smooth hysteresis loops on cooling through the temperature region of ICS manifestation. Toward low temperature,  $P_r$  from both PBLN44/4.0 and PBN44 turns out to be comparable (Fig. 7). In fact, keeping in mind the afore-mentioned sudden and considerable drop of  $E_c$  at 125 K, one may consider acceptable postulating that the PBN44's hysteresis loops transform tending, in comparison with the high-temperature data, to a pseudo-slim-like form (125 K-data in Fig. 6(b)). Revelation of the properly slim-like appearance is in this case most likely frustrated because of the frozen-like ferroelectric state applying toward low temperature and involving, normally, comparatively higher  $E_c$  values, which is a natural trend in ferroelectrics, as commented above. In any case, note that the polarization-temperature behavior observed in Fig. 7 for PBN44 on cooling looks like that from a proper relaxor ferroelectric on heating through the DRPT region [31].

The above results strongly support our advice that development of incommensurate modulation in these materials has here the apparent effect of really frustrating the long-range cooperative alignment of the ferroelectric dipoles and, hence, ferroelectric macrodomains formation. To further enrich this discussion, we chose to process the dielectric data from these materials also in terms of Curie-Weiss law, which establishes that  $\varepsilon' = C/(T - T_{CW})$  above  $T_C$ , where  $C$  is the Curie constant and  $T_{CW}$  the Curie-Weiss temperature. The temperature dependences of reciprocal permittivity of PBN44 and

PBLN44/4.0 are illustrated in Fig. 8, for the 1 kHz data. The data from PBN44 can be to some extent considered as following nearly a Curie-Weiss behavior (i.e., pseudo-normal ferroelectric), while the data from the relaxor PBLN44/4.0 ferroelectric diverge noticeably from this behavior on cooling from a given temperature, known as Burn's temperature ( $T_B$ ), of 621 K. PNRs formation has normally been accepted to essentially start at  $T_B$ , being viewed as responsible for DRPT occurrence in ferroelectrics [8]. In the following, in addition, the Curie-Weiss trend and P-E hysteresis loop characteristics from PBLN44/0.5 were as well investigated, the results being shown in the Fig. 8 inset and Fig. 6(c), respectively. Although this sample presents a non-relaxor ferroelectric to paraelectric phase transition (Fig. 5(a)), note in the Fig. 8 inset that its dielectric data also show, however, a departure from the Curie-Weiss behavior on cooling from a given  $T_B$  value of 620 K. According to Fig. 6(c), moreover, high-temperature slim-like hysteresis loops also apply to this sample, with  $P_r$  showing as well only a moderate and natural increase on cooling (Fig. 7 inset).

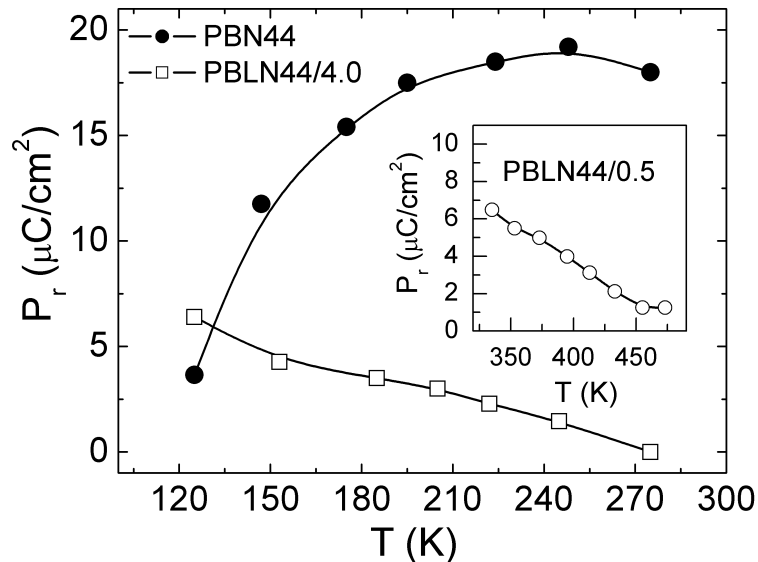


**Figure 7.** Temperature dependences of remnant polarization ( $P_r$ ) for PBN44 and PBLN44/4.0. The data for PBLN44/0.5 are shown in the figure inset.

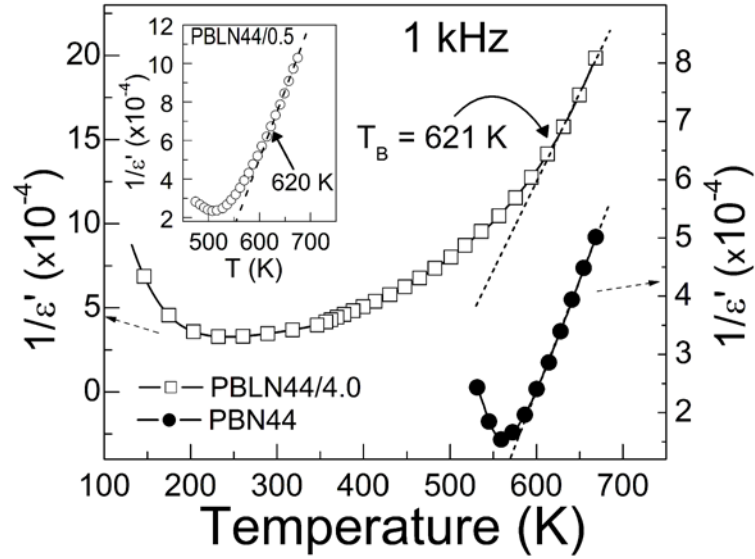


**Figure 8.** Temperature dependences of reciprocal permittivity ( $\epsilon'$ ) for PBN44 and PBLN44/4.0. The data for PBLN44/0.5 are shown in the figure inset.  $T_B$  represents the temperature at which the data diverge from the Curie-Weiss law of linear behavior (with a slope basically equal to the unity), being found reasonable values of  $C = (0.95\text{-}2.61) \cdot 10^5$  K in this study.

All these results allow stating, in association with literature [8,30-32], that  $\text{La}^{3+}$  introduction into PBN should cause sufficient compositional disorder/fluctuations as to favor formation of tiny polar regions, but with a coherency order probably exceeding the nano-scale size, i.e., approaching to reaching the micro-scale local order. These minute regions have essentially non-dynamical nature (at least, within the frequency window explored here), leading to observation, as for PBLN44/0.5, of diffuse but non-relaxor ferroelectric to paraelectric phase transition in PBLN. Meanwhile, development of low-temperature ICS should reduce the size order of the domains coherency and favor formation of dynamical PNRs, inside which polarization fluctuations occur. This fact leads to development, as for PBLN44/4.0, of DRPT in such materials, depending (but truly only) on whether  $T_C$  lies or not within the temperature region of ICS expression after doping. As ICS already appear in  $\text{La}^{3+}$ -free PBN, note here the irrelevance of postulating, for instance, a given critical  $\text{La}^{3+}$  dopant content that would be supposed to provoke

structural disorder strength as sufficient as to particularly induce the materials' relaxor characteristics.

It is not possible to generalize the results of this work to other ferroelectric systems exhibiting diffuse phase transition and relaxor characteristics; nevertheless, the results of Knudsen and coauthors [33] indicate, the presence of an incommensurate antiferroelectric modulation in most grains of relaxor PLZT 4/90/10 and 10/90/10 perovskite structured materials. It is timely to state here, therefore, that although this observation of ICS-induced DRPT in the PBN-based materials does not openly apply to other ferroelectrics, the present results for sure suggest that, in studies aimed at advancing discussion on this topic, some possible causes or mechanisms of DRPT other than compositional/structural disorder in ferroelectric materials should not be straightforwardly ruled out.

#### 4. Conclusions

In this work,  $\text{La}^{3+}$ -doped  $\text{Pb}_{0.56}\text{Ba}_{0.44}\text{Nb}_2\text{O}_6$  (PBN44) ferroelectric electroceramics were prepared and studied from both (micro)structural and dielectric viewpoints. It is shown that  $\text{La}_2\text{O}_3$  doping induces the formation of orthorhombic  $mm2$  phase (coexisting with the original tetragonal  $4mm$  one), which increases with increasing  $\text{La}_2\text{O}_3$  content. In particular, the average grain size and dielectric permittivity show anomalous behaviors for a doping extent of 1 wt.%  $\text{La}_2\text{O}_3$ . It is noted that this percentage leads the original PBN44 material to definitely show (micro)structural characteristics and dielectric properties comparable to those observed in PBN compositions lying within the morphotropic phase boundary region, where the dielectric (ferroelectric and piezoelectric) properties of such materials are well-known to be reasonably enhanced. Finally, it is here proposed that the crossover from normal to diffuse plus relaxor phase transition (DRPT) in  $\text{La}^{3+}$ -doped PBN44 ferroelectrics is directly linked with the incommensurate superstructures (ICS) that



naturally develop in PBN materials toward low temperatures. Concretely, our results show that the dopant favors occurrence of diffuse but really not relaxor phase transition in these materials. Instead, conversion to DRPT materializes depending only on whether the phase transition temperature finally lies or not within the temperature region of ICS manifestation, these superstructures exhibiting originally an intrinsically frequency-dispersive dielectric response.

### **Acknowledgements**

This work was supported by FAPESP and CNPq, two Brazilian research-funding agencies. Support from MAT2010-21088-C03-02 research project of the Spanish Government is also grateful. The authors gratefully acknowledge technical assistance from Francisco J. Picon. J. E. García wishes to thank Erasmus Mundus External Cooperation Window EU-Brazil Startup project and JPI-2012 Santander-Universidades program for their financial support.

## References

- [1] Jaffe B, Cook WR and Jaffe H (1971) *Piezoelectric Ceramics*. Academic, England.
- [2] Uchino K (2000) *Ferroelectrics Devices* 2nd ed. Taylor and Francis Group, USA.
- [3] Goodman G (1953) Ferroelectric properties of lead metaniobate, *J. Am. Ceram. Soc.* 36:368-372.
- [4] Francombe MH (1960) The relation between structure and ferroelectricity in lead barium and barium strontium niobates, *Acta Cryst.* 13:131-140.
- [5] Guo R, Bhalla AS, Randall CA, Chang ZP and Cross LE (1990) Polarization mechanisms of morphotropic phase-boundary lead barium niobate (PBN) compositions, *J. Appl. Phys.* 67:1453-1460.
- [6] Cross LE (1987) Relaxor ferroelectrics, *Ferroelectrics* 76:241-267.
- [7] Singh G, Tiwari VS and Wadhawan VK (2001) Crossover from relaxor to normal ferroelectric behavior in  $(1-x)\text{Pb}(\text{Mg}_{1/3}\text{Nb}_{2/3})\text{O}_3-x\text{PbZrO}_3$  ceramic near  $x=0.5$ , *Solid State Commun.* 118:407-411.
- [8] Bokov AA and Ye ZG (2006) Recent progress in relaxor ferroelectrics with perovskite structure, *J. Mater. Sci.* 41:31-52.
- [9] Rivera I, Kumar A, Ortega N, Katiyar RS and Lushnikov S (2009) Divide line between relaxor; diffused ferroelectric; ferroelectric and dielectric, *Solid State Commun.* 149:172-176.
- [10] Venet M, Vendramini A, Garcia D, Eiras JA and Guerrero F (2006) Tailoring of the lead metaniobate ceramic processing, *J. Am. Ceram. Soc.* 89:2399-2404.
- [11] R. Neurgaonkar R, Oliver JR, Nelson JG and Cross LE (1991) Piezoelectric and ferroelectric properties of La-modified and unmodified tungsten bronze  $\text{Pb}_{0.6}\text{Ba}_{0.4}\text{Nb}_2\text{O}_6$  dense ceramics, *Mat. Res. Bull.* 26:771-777.
- [12] Venet M, Zabotto FL, Eiras JA and Garcia D (2009) Improvement of the phase diagram for the pseudobinary  $\text{PbNb}_2\text{O}_6 - \text{BaNb}_2\text{O}_6$  system, *J. Appl. Phys.* 105:124106.
- [13] Venet M, A. Eiras J and Garcia D (2009) Anisotropic properties in textured lead barium niobate compositions around the morphotropic phase boundary, *Solid State Ionics* 180:320-325.
- [14] Dai X and Viehland D (1994) Effects of lanthanum modification on the antiferroelectric ferroelectric stability of high zirconium content lead zirconate titanate, *J. Appl. Phys.* 76:3701-3709.

- [15] Gupta SM, Li J-F and Viehland D (1998) Coexistence of Relaxor and Normal Ferroelectric Phases in Morphotropic Phase Boundary Compositions of Lanthanum-Modified Lead Zirconate Titanate, *J. Am. Ceram. Soc.* 81:557-564.
- [16] Barranco AP, Guerra JDS, Zaldívar OG, Piñar FC, Araújo EB, Hall DA, Mendoza ME and Eiras JÁ (2008) Effects of lanthanum modification on dielectric properties of  $\text{Pb}(\text{Zr}_{0.90}\text{Ti}_{0.10})\text{O}_3$  ceramics: enhanced antiferroelectric stability, *J. Mater. Sci.* 43:6087-6093.
- [17] Tang B, Fan H, Ke S and Liu L (2007) Microstructure evolutions and electrical properties of  $\text{Pb}_{1-x}\text{La}_x(\text{Zr}_{0.56}\text{Ti}_{0.44})_{1-x/4}\text{O}_3$  ceramics, *Mater. Sci. Eng., B.* 138:205-209.
- [18] Dai X, Xu Z and Viehland D (1994) The Spontaneous Relaxor-to-Normal Ferroelectric Transformation in La-Modified Lead Zirconate Titanate, *Philos. Mag. B.* 70:33-48.
- [19] Li JF, Dai X, Chow A and Viehland D (1995) Polarization Switching Mechanisms and Electromechanical Properties of La-Modified Lead Zirconate Titanate Ceramics, *J. Mater. Res.* 10:926-938.
- [20] Thomas NW (1983) A New Framework for Understanding Relaxor Ferroelectrics, *J. Phys. Chem. Solids*, 51:1419-1431.
- [21] Venet M, M'Peko JC, Zabotto FL, Guerrero F, Garcia D and Eiras JA (2009) Dynamics of normal to diffuse and relaxor phase transition in lead metaniobate-based ferroelectric ceramics, *Appl. Phys. Lett.* 94:172901.
- [22] Randall CA, Guo R, Bhalla AS, Cross LE and relations in tungsten bronze lead barium niobate (1991)  $\text{Pb}_{1-x}\text{Ba}_x\text{Nb}_2\text{O}_6$ , *J. Mater. Res.* 6:1720-1728.
- [23] Xu Y, Li Z, Li W, Wang H and Chen H (1989) Phase-transition of some ferroelectric niobate crystals with tungsten-bronze structure at low-temperatures, *Phys. Rev. B* 40:11902-11908.
- [24] Guerra JDS, Venet M, Garcia D and Eiras JA (2007) Dielectric properties of  $\text{PbNb}_2\text{O}_6$  ferroelectric ceramics at cryogenic temperatures, *Appl. Phys. Lett.* 91:062915.
- [25] Bursill LA and Lin PJ (1986) Chaotic states observed in strontium barium niobate, *Philos. Mag. B* 54:157-170.
- [26] Lin PJ and Bursill LA (1987) Superlattice structure of ferroelectric barium sodium niobate (BNN), *Acta Cryst. B* 43:504-512.
- [27] Lee H-Y and Freer R (1998) High-order incommensurate modulations and incommensurate superstructures in transparent  $\text{Sr}_{0.6}\text{Ba}_{0.4}\text{Nb}_2\text{O}_6$  (SBN40) ceramics, *J. Appl. Cryst.* 31:683-691.

- [28] Levin I, Stennett MC, Miles GC, Woodward DI, West AR and Reaney IM (2006) Coupling between octahedral tilting and ferroelectric order in tetragonal tungsten bronze-structured dielectrics, *Appl. Phys. Lett.* 89:122908.
- [29] Viehland D, Li JF, Jang SJ, Cross LE and Wuttig M (1991) Dipolar-glass model for lead magnesium niobate, *Phys. Rev. B* 43:8316-8320.
- [30] Dai X, Xu Z and Viehland D (1996) Normal to relaxor ferroelectric transformations in lanthanum-modified tetragonal-structured lead zirconate titanate ceramics, *J. Appl. Phys.* 79:1021-1026.
- [31] Viehland D, Jang SJ and Cross LE (1990) Freezing of the polarization fluctuations in lead magnesium niobate relaxors, *J. Appl. Phys.* 68:2916-2921.
- [32] Randall CA, Balha AS, Shrout TR and Cross LE (1990) Classification and consequences of complex lead perovskite ferroelectrics with regard to b-site cation order, *J. Mater. Res.* 5:829-834.
- [33] Knudsen J, Woodward DI and Reaney IM (2002) Domain variance and superstructure across the antiferroelectric/ferroelectric phase boundary in  $\text{Pb}_{1-1.5x}\text{La}_x(\text{Zr}_{0.9}\text{Ti}_{0.1})\text{O}_3$ , *J. Mater. Res.* 18:262-271.